# Intermittent recycle-integrated reactor-separator for production of well-defined non-digestible oligosaccharides from oat β–glucan

Nguyen Hoang S.H., Kaspereit Malte, Sainio Tuomo



**DOI:** 10.1016/j.cej.2020.128352

# Intermittent recycle-integrated reactor-separator for production of well-defined non-digestible oligosaccharides from oat $\beta$–glucan

Hoang S.H. Nguyen [a], Malte Kaspereit [b], Tuomo Sainio [a,*)]

[a] Lappeenranta-Lahti University of Technology LUT, School of Engineering Science, Mukkulankatu 19, 15210 Lahti, Finland

[b] Institute of Separation Science & Technology, Friedrich-Alexander University Erlangen-Nürnberg; Egerlandstraße 3, 91052 Erlangen, Germany

*) Corresponding author. Email: Tuomo.sainio@lut.fi. Tel.: +358-403578638

**Abstract**

A recycle-integrated reactor-separator system was studied experimentally and based on simulations for the acid-catalyzed depolymerization of oat beta-glucan polysaccharide. The aim was to produce oligosaccharides with degree of polymerization in a narrow range (*DP* = 15–30). The reactor was operated intermittently at 80 °C. Batch chromatography with Sephadex G–25 size-exclusion gel was found suitable for the separation of product from reactants and impurities. Part of the reaction mixture was periodically withdrawn and fed to the separation column. Molar mass distributions in four chromatographic fractions (waste, recycle, product, impurities) were monitored with SEC–MALLS. Experiments with 4 h mean residence time showed that the reactor-separator achieved approximately 2.0 and 2.5 times higher yield and purity of target *DP* than a batch reactor. Dimensionless operating parameters and equipment design parameters were introduced for analyzing performance of intermittent reactor-separators. The simulations show that intermittent operation offers higher yield and product purity than continuous operation (CSTR and chromatographic separation) when mean residence time in the reactor is long. Continuous operation is better when productivity is maximized by using short mean residence time and low yield.

**Keywords:** reactor-separator; integrated process; depolymerization; beta-glucan, non-digestible oligosaccharides

## 1. Introduction

Cereal *β*–glucans are soluble dietary fibers mainly found from oat or barley. These particular *β*–glucans are linear polysaccharides composed of up to thousands of D-glucose monomers linked by *β*–(1,3) and *β*–(1,4) glycosidic bonds [1,2]. Nowadays, *β*–glucans are widely used around the globe, for instance, in dairy products and beverages. A growing interest in

*β*–glucans-derived products is due to their health benefits that include not only the cholesterol-lowering effects but also the attenuation of postprandial glycemic response [2–5]. Oat *β*–glucan's ability to increase digesta viscosity in the gastrointestinal tract, hence to delay nutrition absorption from the gut is believed to be a key factor responsible for those health benefits [2,5], even though the direct evidence for a role of viscosity has not been demonstrated.

The effectiveness of health benefits mentioned above is linked to oat *β*–glucan's high viscosity, mainly caused by its high molecular weight ($M_w$) [2,4,6,7]. Nevertheless, a production of oat *β*–glucan with high $M_w$ is not a scope of this work, because they are readily available at high $M_w$ [8]. Instead, the present paper aims to address a production of oat *β*–glucan-derived short polysaccharides and oligosaccharides that are generally considered as non-digestible oligosaccharides. Since non-digestible oligosaccharides are resistant to digestion and absorption in the stomach and small intestine, they reach the large intestine and are fermented by colonic bacteria into short chain fatty acids (SCFA) and lactate plus gases [9,10]. Lower pH caused by SCFA formation could hinder the growth of pathogens, while stimulate the growth of beneficial bacteria, mainly Bifidobacteria species [11]. Also, they are low in sweetness and caloric values [9–11].

Several non-digestible oligosaccharides have been studied and commercialized [12]. Among them, fructo- and galacto-oligosaccharides are the most popular ones. To the best of our knowledge, a production of non-digestible oligosaccharides with controlled *DP* derived from oat *β*–glucans has not been studied. In fact, there are no commercial products, for instance, with *DP* ranging from 15 to 30, although these were reported to have the most profound immunological effects [13]. There are two main reasons for such rarity. Firstly, a production *β*–glucan with well-defined *DP* via hydrolysis is challenging because a hydrolysate normally

contains a very broad variety of molecules with *DP* from 1 up to thousands depending on a starting material [1,14]. Secondly, *β*–glucan with low $M_w$ and well-defined *DP* is even more difficult to be synthesized because hydrolysis would need to be performed in a highly controlled manner so that polysaccharides would not be completely degraded to monomers.

In a recent study [15], hydrolysates ($\overline{M_w}$ = 4150–4500 g/mol ~ $\overline{DP}$ = 26–28) of oat *β*–glucan produced from acid and oxidative degradation were found to have several positive effects. Typically, fat and bile binding capacities were found to increase significantly after degradation both by acid and oxidative agent. More specifically, hydrolysate prepared by acid possesses high fat binding capacity, whereas oxidative degradation results in higher bile binding capacity [15]. Both degradation methods significantly increase antioxidant and antibacterial activities [15]. The findings are found interesting because *DP* of hydrolysates prepared is within a range aimed in the current research (*DP* = 15–30).

While it is possible to produce oligosaccharides with desired *DP* by a stand-alone reactor, for instance, a batch reactor [14,16,17], the main limitation of the stand-alone reactor is that purity (regarding the presence of molecules larger or smaller than the desired molecular weight distribution) and yield are deemed low because the effluent contains not only target components but also unreacted reactants and too small molecules. The separator (*e.g.*, membrane or chromatographic column) could be used after the reactor to increase purity, but not yield.

To further improve purity and yield, the most common approach is an integration of reactor and separator units [18], which could be a fully-integrated or recycle-integrated reactor-separator system. In the former (*e.g.*, membrane reactor [19–21]), the reaction and separation

occur in the same physical unit. In the latter [18,22–24], the reaction is carried out in a reactor. The stream from the reactor is transferred to a separation unit, where the desired components are collected. At the same time, the others (unreacted reactants and catalysts) are recycled back to the reactor, and too small molecules are withdrawn.

A membrane unit appears to be the most common choice as a separator [19–23], because it is straightforward to operate, and an integrated system could be operated continuously. However, it comes with a limitation that a molecular mass distribution (MMD) of oligosaccharides may remain broad unless a cascade of membranes with different molecular weight cut-off (MWCO) is used. A size-exclusion chromatography (SEC) column is a better choice for more narrow size distribution. In one study, a direct comparison between diafiltration and SEC for recovery of hemicellulose was investigated. It was reported that SEC offers higher purity and recovery (82% and 99%, respectively) than diafiltration (77% and 87%, respectively). The authors argued that diafiltration is dependent on the purity of feed solution, which was highly contaminated by low molecular weight compounds, whereas SEC is not affected [25]. But it is worth noting that the concentration of product from SEC is rather low due to dilution.

In this study, an intermittent recycle-integrated reactor-separator (hereafter referred to as RS) is investigated experimentally and by means of mathematical modeling for producing non-digestible oligosaccharides from oat $\beta$–glucan. A preparative SEC column is chosen over a membrane as a separator because it is expected to provide better purity towards desired molecules. “Intermittent” reflects the nature of the process in the experimental setup, where a solution is periodically withdrawn from a reactor and fed into the SEC column. In this work, reactor-separator is analyzed using dimensionless designing and operating parameters, which allows the integrated system to mimic either a continuous or a batch operation mode. The

structured kinetic model reported previously [1,14] is used to describe the acid-catalyzed hydrolysis of oat *β*–glucans in the reactor. An efficient model for the preparative SEC is developed based on discrete convolution. The study is expected to serve as a theoretical guide to produce well-defined polysaccharides or oligosaccharides with controlled *DP* from oat *β*–glucans, including but not limited to *DP* = 15–30. The models used in this work are flexible enough to enable predicting the formation of polysaccharides and oligosaccharides with any size.

## 2. Experimental methods

Oat *β*–glucan solution (medium viscosity, purity > 94%, Megazyme, Ireland) was dissolved in deionized water by stir-heating at 70–80 °C. The solution was kept refrigerated at 4 °C prior to experiments. Other chemicals used were analytically graded.

### *2.1. Hydrolysis experiments*

Acid hydrolysis of oat *β*–glucan was carried out in 50 mL jacketed glass reactor using HCl as a catalyst. The temperature was monitored. The oat *β*–glucan solution ($V$ = 45 mL, $c$ ~ 4.76 g/L) was preloaded in the reactor and heated while stirring (400 rpm). When the solution reached 80 °C, the reaction was started by adding HCl solution ($V$ = 5 mL, $c_{HCl}$ = 0.5 M) into the reactor. The initial concentration of *β*–glucan was $c_{BG}^{0}$ ~ 4.284 g/L and the catalyst concentration was $c_{HCl}$ = 0.05 M.

Four samples ($t$ = 120, 200, 250, and 360 min, 10 mL each) were collected into 10 mL PTFE tubes and quickly cooled in an ice-water bath and neutralized by NaOH. These hydrolysates were used to calibrate a column model of size-exclusion chromatographic separation.

### *2.2. Preparative size-exclusion chromatographic separation*

The preparative SEC column (L × I.D. 70 cm × 1.5 cm) was packed by Sephadex G–25 medium (particle size: 50–150 μm, swelling factor ~ 1.7). The injection was performed with an injection loop that was filled by a hydrolyzed solution using a syringe. The separation was performed at 60 °C with degassed ultrapure water as the eluent at a flow rate of 0.5 mL/min.

### *2.3. Intermittent recycle-integrated reactor-separator*

The intermittent recycle-integrated reactor-separator system used in this work is illustrated in Fig. 1. Its operation is characterized by periodic withdrawal of a part of the reaction solution, separation of the latter by SEC, and re-introduction of fractions with insufficient conversion into the reactor, along with introduction of fresh feed and catalyst. The details of experiments that contain volumes of solutions withdrawn, introduced, and injected as well as the corresponding time values are presented in Table S1 and S2. The volumes of solutions were calculated by dividing their recorded mass by density (Anton Paar DMA 4500 M).

The reactor and separator units were equilibrated at operating temperatures overnight prior to experiments. Hydrolysis reaction was performed at 80 °C in a jacketed glass reactor and HCl was used as a catalyst. The reactor was pre-filled by the fresh oat $\beta$–glucan solution and stirred at 400 rpm. When the solution reached 80 °C, HCl solution was introduced into the reactor and time set as zero. After 60 min (column 10, Table S1), solution was withdrawn from the reactor

(column 11, Table S1). At the same time, HCl solution, fresh oat *β*–glucan, and recycle fraction from the separator (column 3, 5, and 6, respectively, Table S1) were fed to the reactor. The amount of acid solution added was adjusted by a pH meter. The withdrawn hydrolysate was injected into the column by using a syringe (column 4, Table S2). A recycle fraction was collected by a fraction collector (column 5 and 6, Table S2). The fractionation mode in the experimental work is illustrated in Fig. S1. In total, seven cycles of reaction and separation were carried out for a demonstration.

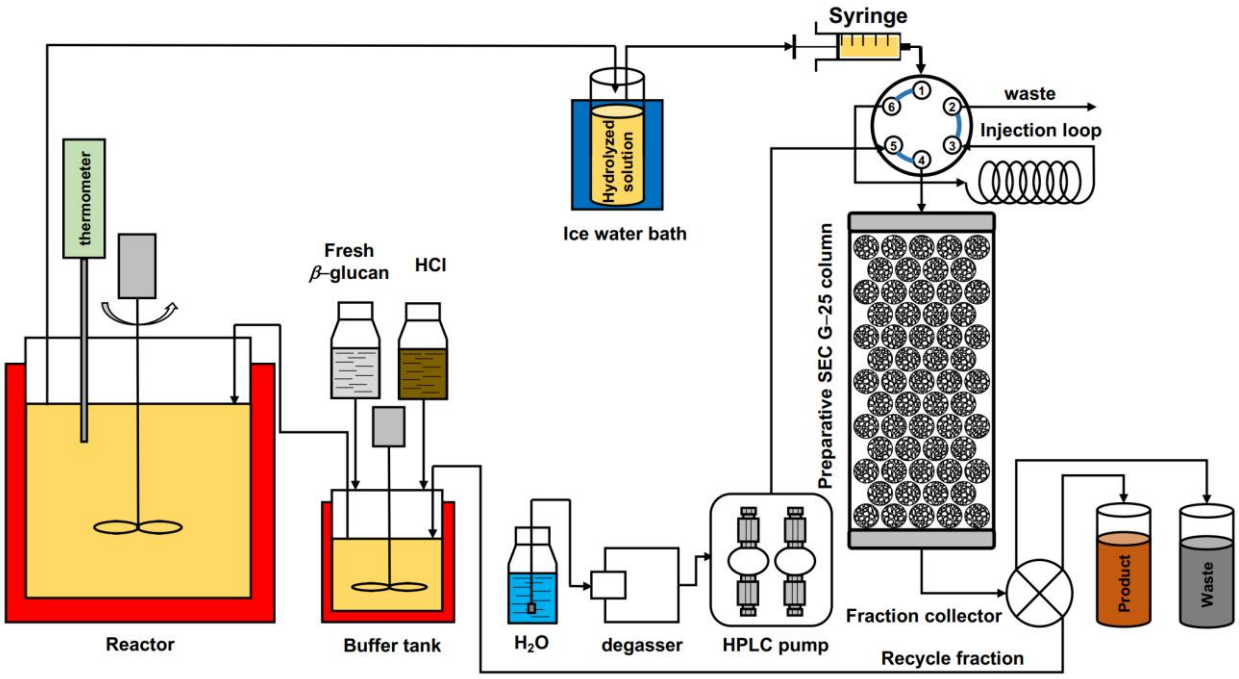


**Figure 1.** Experimental setup of the intermittent recycle-integrated reactor-separator system

### *2.4. Analysis*

Samples collected from the preparative SEC column (hereafter referred to as fractions) were analyzed by analytical size-exclusion chromatography coupled to multiangle laser light scattering (SEC–MALLS) to determine molar mass distribution (MMD). The SEC–MALLS

analysis was performed on an Agilent 1200 Infinity series equipped with an RI detector and miniDAWN TREOS (Wyatt Technology, USA) MALLS detector. Two columns connected in series were used – a TSKgel SuperMultiporePW–M column (L × I.D. 15 cm × 6 mm, $M_w$ range = $5\times10^2 - 1\times10^6$ g/mol, Tosoh Bioscience, Germany) and a TSKgel G–Oligo–PW column (L × I.D. 30 cm × 7.8 mm, $M_w < 3\times10^3$ g/mol, Tosoh Bioscience, Germany) maintained at 60 °C. The eluent was an aqueous NaCl solution ($c_{NaCl}$ = 0.08 M) degassed and pumped at 0.4 mL/min.

Fractions (1.8 mL each) collected from the preparative SEC column were filled with NaCl 1 M ($V$ ~ 50 – 200 μL) to yield $c_{NaCl}$ ~ 0.08 M. Prior to injection (100 μL), fractions were filtered by using syringe filters (Phenomenex, 0.2 μm). The refractive index increment (d$n$/d$c$) of 0.146 was set for *β*–glucan in calculations [26–28]. MMD was determined by the ASTRA software (version 6.1.2).

## 3. Mathematical models and numerical simulation methods

### *3.1. Kinetics of acid-catalyzed hydrolysis of oat β–glucan*

A structured kinetic model developed previously was used to model the hydrolysis reaction kinetics [1,14]. The model takes into account the difference in reactivity of *β*–(1,4) and *β*–(1,3) glycosidic bonds, which was found to be statistically significant. Also, the dependence of glycosidic bonds' reactivity on their position in the polysaccharide chain is taken into account. Eq. (1) describes the reactivity of glycosidic bonds decreasing with the distance from the nearest chain end

$$k_j(\delta) = k_j^0\left(\alpha + \frac{1-\alpha}{\delta^\beta}\right) \quad (1)$$

where $k_j$ is the reaction rate constant for acid-catalyzed hydrolytic cleavage of $\beta$–(1,4) or $\beta$–(1,3) glycosidic bond at position $\delta$ counting from the nearest chain end. $k^0$ is the reactivity at the chain end, and $\alpha$ and $\beta$ are dimensionless adjustable parameters. The values of parameters were taken from the previous study [14].

### *3.2. Size-exclusion chromatographic separation*

**Column model**

The mass balance for a species $j$ in a chromatographic separation column can be written as in Eq. (2)

$$\varepsilon_b \frac{\partial c_j}{\partial t} + (1-\varepsilon_b)\frac{\partial c_{s,j}}{\partial t} + \frac{Q}{A_{col}}\frac{\partial c_j}{\partial z} = \varepsilon_b D_{ax,j}\frac{\partial^2 c_j}{\partial z^2} \quad (2)$$

where $c_j$ and $c_{s,j}$ are the concentration of a component in the mobile and stationary phase, respectively. $Q$ is the volumetric flow rate and $D_{ax,j}$ is the axial dispersion coefficient of component $j$ in the mobile phase. A is the cross-sectional area of the column. The volume fraction of liquid between the particles in the bed (bed porosity) is denoted by $\varepsilon_b$ and determined by injecting a high molecular mass substance that is unable to penetrate the pores. In this work, blue dextran ($M_w = 2\times10^6$ g/mol) was used to determine $\varepsilon_b$.

Generally in a multicomponent system, the concentrations $c_j$ are linked through a phase equilibrium function $c_{s,j} = f(c_1, c_2, \ldots c_N)$. In the present case, *i.e.*, size-exclusion chromatography of molecules with weak interactions with the stationary phase, the distribution of species $j$ between liquid and solid phases can be regarded linear and independent of the other components. If the solution in the pores of the stationary phase is always in equilibrium with the liquid between the particles, the mass balance becomes

$$\frac{\partial c_j}{\partial t}\left(\varepsilon_b + (1-\varepsilon_b)H_j\right) + \frac{Q}{A_{col}}\frac{\partial c_j}{\partial z} = \varepsilon_b D_{ax,j}\frac{\partial^2 c_j}{\partial z^2} \quad (3)$$

where the distribution is given by $H_j$, the slope of the linear isotherm $c_{s,j} = H_j c_j$. The material balance can be rewritten as

$$\frac{\partial c_j}{\partial t} + \frac{u}{\bar{\varepsilon}_j}\frac{\partial c_j}{\partial z} = \bar{D}_j\frac{\partial^2 c_j}{\partial z^2} \quad (4)$$

where the linear velocity $u = Q/A_{col}$ and the apparent porosity and axial dispersion coefficient are related to the physical quantities by

$$\bar{\varepsilon}_j = \varepsilon_b + (1-\varepsilon_b)H_j \quad (5)$$

$$\bar{D}_j = \frac{D_{ax,j}}{1 + \frac{1-\varepsilon_b}{\varepsilon_b}H_j} \quad (6)$$

With these definitions, Eq. (4) can be interpreted as flow of species *j* in an empty tube at a linear flow rate $u_j = u/\bar{\varepsilon}_j$ and with an apparent axial dispersion coefficient $\bar{D}_j$. Since $H_j$ decreases with increasing molecular size, the empty tube linear flow rate and axial dispersion coefficient are higher for large polysaccharides than for smaller polysaccharides.

Eq. (4) can be solved numerically by using one of the methods that transform the partial differential equations (PDE) to a system of ordinary differential equations (ODE). In the present system, there are hundreds or thousands of individual molecules and a more efficient approach is needed. Here we use the well-known analytical solution for the residence time distribution for axially dispersed turbulent flow in an empty tube and construct the chromatograms by using the convolution method as will be described below. The residence

time distribution function (in the case of moderate dispersion, $DL/u < 0.01$) in an empty tube can be calculated as [29]

$$E_j(t) = \sqrt{\frac{u^3}{4\pi\bar{\varepsilon}_j^3 \bar{D}_j L}} \exp\left[ -\frac{\left( L - \frac{ut}{\bar{\varepsilon}_j} \right)^2}{4\bar{\varepsilon}_j \bar{D}_j L/u} \right] \quad (7)$$

where $L$ is the height of the column. The subscript $j$ is used to clarify that the residence time distribution depends on molecular size. The apparent dispersion coefficient can be expressed using the number of theoretical stages concept, $NTP$, as [30]

$$\bar{D}_j = \frac{Lu}{2\bar{\varepsilon}_j NTP_j} \quad (8)$$

and Eq. (7) can thus be rewritten as

$$E_j(\tau) = \frac{u}{\bar{\varepsilon}_j L} \sqrt{\frac{NTP_j}{2\pi}} \exp\left[ -\left( 1 - \frac{\tau}{\bar{\varepsilon}_j} \right)^2 \frac{NTP_j}{2} \right] \quad (9)$$

where $\tau = ut/L$ is a dimensionless time.

## Numerical implementation

Size-exclusion chromatography (SEC) can be considered as a linear time-invariant system (LTI) [31,32]. The output signal is the chromatogram at the column outlet. It is obtained by the convolution of the inlet signal and the residence time function. In other words, $C_{\text{out},j}$ is the convolution of $E_j$ with $C_{\text{in},i}$ as shown in Eq. (10), where the asterisk is the convolution operator. The injection profiles were assumed to be rectangular in the absence of other information.

$$C_{\text{out},j}(t) = E_j(t) * C_{\text{in},j}(t) \quad (10)$$

Since convolution can be conveniently performed based on fast Fourier transform and its inverse, numerical solution is obtained using standard calculation packages. For example, in Matlab®, the convolution can be performed simply as

$$C_{\mathrm{out},j}(t) = \mathtt{ifft}\left(\mathtt{fft}\left(E_j\ (t)\right) \times \mathtt{fft}\left(C_{\mathrm{in},j}(t)\right)\right) \tag{11}$$

**Parameters of the residence time and dispersion models**

As seen in Eq. (9), the response of the SEC column is governed by two parameters, namely the apparent porosity $\bar{\varepsilon}_j$ and number of theoretical stages $NTP_j$. It is straightforward to calculate the apparent porosity from the retention volume of a single solute. Because monodisperse polysaccharides are not readily available, however, a different approach was adopted. Polydisperse solutions of oat $\beta$–glucans were prepared by acid hydrolysis in a batch reactor ($T$ = 80 °C, $c_{\mathrm{HCl}}$ = 0.05 M). Using different reaction times (120, 200, 250, and 360 min) lead to different $M_{\mathrm{w}}$ distributions in the range of 1,000 < $M_w$ < 100,000 g/mol. Each batch was fed to the preparative SEC column (Sephadex G–25), and up to 20 fractions were collected from the outlet in each run. The chromatogram for each $DP$ was determined by analyzing collected fractions using analytical SEC–MALLS as described Section 2.4. Finally, $\bar{\varepsilon}_j$ was calculated from the first moment of the corresponding chromatogram.

Two empirical models were used to correlate the variation of $\bar{\varepsilon}_j$ with $M_w$. Model I, Eq. (12), is a modified Gompertz function with $a$, $b$, $c$, and $d$ as adjustable parameters.

$$\bar{\varepsilon}_j = a\left(1 - b\exp\left(-c\exp\left(-d\times\log_{10}\left(M_{w,j}\right)\right)\right)\right) \tag{12}$$

Model II was derived from an extended Ogston model [33]. In Eq. (13), $\lambda$ is a parameter related to the volume fraction of polymer in the swollen gel and $\gamma$ and $\omega$ are adjustable parameters.

$$\bar{\varepsilon}_j = \varepsilon_b + (1-\varepsilon_b)\exp\left(-\left(1+\gamma M_{w,j}^{\omega}\right)\ln\lambda\right) \quad (13)$$

An empirical correlation, Eq. (14), was used to relate *NTP* to molar mass

$$NTP_j = \varphi \times M_{w,j}^{-\sigma} \quad (14)$$

The constants $\varphi$ and $\sigma$ were estimated by fitting calculated chromatograms to experimental chromatograms of four oat $\beta$–glycan hydrolysates obtained in a batch reactor with reaction times $t$ = 120, 200, 250, and 360 min. NTP values determined experimentally for very small (glucose) and very large (Blue Dextran) molecules were included in the parameter estimation.

### *3.3. Process design*

The intermittent reactor–separator process was analyzed using three parameters. The equipment configuration was characterized by a dimensionless parameter $\nu$, which was defined as the volume ratio of the reactor, $V_R$, to the separation column, $V_{col}$

$$\nu = \frac{V_R}{V_{col}} \quad (15)$$

According to the intermittent operation strategy, a certain volume of solution was periodically withdrawn from the reactor and fed into the separation column. A dimensionless operating parameter $\phi$ was used to quantify the volume of the fraction of solution was withdrawn on each cycle. It was defined by using $V_{col}^{F}$, the volume of feed into the SEC column, as in Eq. (16)

$$\phi = \frac{V_{col}^{F}}{V_R} \quad (16)$$

It is observed from Eqs. (15) and (16) that the volumetric loading of the column can be calculated from these dimensionless parameters as $V_{\mathrm{col}}^{\mathrm{F}}/V_{\mathrm{col}} = \phi\nu$ .

Besides $\phi$ and $v$, the performance of the reactor–separator depends on the cycle time, $t_{\mathrm{cycle}}$. It was assumed that the duration of the separation is not a limiting factor, and the time between consecutive withdrawals from the reactor can be chosen freely. To compare the intermittent reactor–separator with a continuous one, *i.e.*, a reactor–separator with a CSTR coupled with a SEC separation column, the mean residence times in the two reactors must be equal. Since a volume fraction $\phi$ is withdrawn and replaced by a fresh solution at intervals of $t_{\mathrm{cycle}}$, the mean age of volume elements in the reactor at the end of cycle $N$ becomes

$$t_{\mathrm{mean}} = \phi t_{\mathrm{cycle}} + (1-\phi)\phi 2t_{\mathrm{cycle}} + (1-\phi)^2 \phi 3t_{\mathrm{cycle}} + \ldots + (1-\phi)^{N-1} \phi N t_{\mathrm{cycle}} \tag{17}$$

At steady state, the mean exit age is

$$t_{\mathrm{mean}} = t_{\mathrm{cycle}} \sum_{k=1}^{\infty} k\phi(1-\phi)^{k-1} = \frac{t_{\mathrm{cycle}}}{\phi} \tag{18}$$

and, since the mean age in a CSTR equals the space-time $\tau_{\mathrm{CSTR}}$, the intermittent and continuous reactor-separators are comparable when

$$t_{\mathrm{cycle}} = \phi\tau_{\mathrm{CSTR}} \tag{19}$$

### *3.4. Evaluation of process performance*

Short polysaccharides with *DP* in the range of 15 to 30 were chosen as the target molecules. Molecules above this range were regarded as reactants and those below this range as impurities. Purity is the mass fraction of target molecules in the product fraction

$$Pu = \frac{m_{\text{target}}^{\text{P}}}{m_{\text{tot}}^{\text{P}}} \tag{20}$$

Yield is defined as the mass of target molecules in the product fraction relative to the mass of fresh oat $\beta$–glucan (BG) introduced as fresh feed (superscript FF) on each cycle.

$$Y = \frac{m_{\text{target}}^{\text{P}}}{m_{\text{BG}}^{\text{FF}}} \tag{21}$$

Specific productivity is defined here based on equipment volume and time-average flow of the target molecules out of the intermittent process. Separators are often more expensive to construct and operate than reactors, except for when expensive catalysts are needed. In order to include the effect of separation costs without using case-specific numerical values, the volume of the separator is multiplied by a relative cost factor $\chi$. Specific productivity then becomes

$$PR = \frac{Ym_{\text{BG}}^{\text{FF}}}{t_{\text{cycle}}\left(V_{\text{R}} + \chi V_{\text{col}}\right)} = \frac{Yc_{\text{R,BG}}^{0}}{t_{\text{mean}}}\frac{\nu}{\chi + \nu} \tag{22}$$

Here $c_{\text{R}}^{0}$ is the mass concentration of oat $\beta$–glucan in the reactor at the beginning of the cycle when $\phi = 1$.

## 4. Results and discussion

### *4.1. Size-exclusion chromatographic separation*

The preparative SEC column was characterized by feeding small amounts of small carbohydrates (glucose, cellobiose) and a large dextran polymer. The maximum separation factor was calculated to be approximately 2.0. The apparent porosity and number of theoretical plates of these substances (Table 1), calculated directly from the experimental chromatograms, can be regarded as the upper and lower boundaries for the correlations in Eqs. (12) to (14).

**Table 1.** $\bar{\varepsilon}$ and NTP of glucose, cellobiose and blue dextran

| **Compound** | $M_w$ **(g/mol)** | $\bar{\varepsilon}$ | ***NTP*** |
|---|---|---|---|
| Glucose | 180.16 | 0.783 | 965 |
| Cellobiose | 342.3 | 0.741 | 828 |
| Blue dextran | $2\times10^6$ | 0.389 | 323 |

The apparent porosities for molecules of various sizes, calculated from pulse experiments with $\beta$–glucan hydrolysates, are displayed in Fig. 2A. The results obtained with hydrolysates of varying reaction time are consistent, except for a small variation in the apparent porosity of the largest molecules. The $t$ = 120 min hydrolysate is mostly composed of molecules in the range 7 500 < $M_w$ < 65 000 g/mol), and $\bar{\varepsilon}$ ranges from 0.40 to 0.42. Molecules with $M_w$ > 65 000 g/mol were largely hydrolyzed already at $t$ = 120 min and were present only in small amounts. The molar masses in the $t$ = 200 min and $t$ = 250 min hydrolysates are quite similar (4 000 < $M_w$ < 40 000 g/mol), with the apparent porosity in the range of 0.42 to 0.48. In the batch hydrolyzed for 360 min, the molar mass range 2 500 < $M_w$ < 4 000 g/mol is close to the target size. Their apparent porosity ranged from 0.46 to 0.53, indicating that separation from the reactants should be possible.

A characteristic feature of the experimentally determined $\bar{\varepsilon}$ is that it reaches a lower limit (equal to the bed porosity $\varepsilon_b$) at approximately 10 000 g/mol and is constant for larger molecules. Both Model I (the modified Gompertz function in Eq. (12)) and Model II (based on the Ogston model, Eq. (13)) can reproduce this behavior. However, Model I is significantly more accurate in this range ($R^2$ = 95.67% vs $R^2$ = 85.52%). On the other hand, Model I predicts a nearly constant value for $\bar{\varepsilon}$ at $M_w$ < 900 g/mol, which is not in agreement with experimental

observations. Considering that the highest precision is needed at the $M_w$ = $10^3$ – $10^5$ g/mol range (Fig. 2A), Model I is chosen. The best-fit parameters estimated for the two models are given in Table 2.

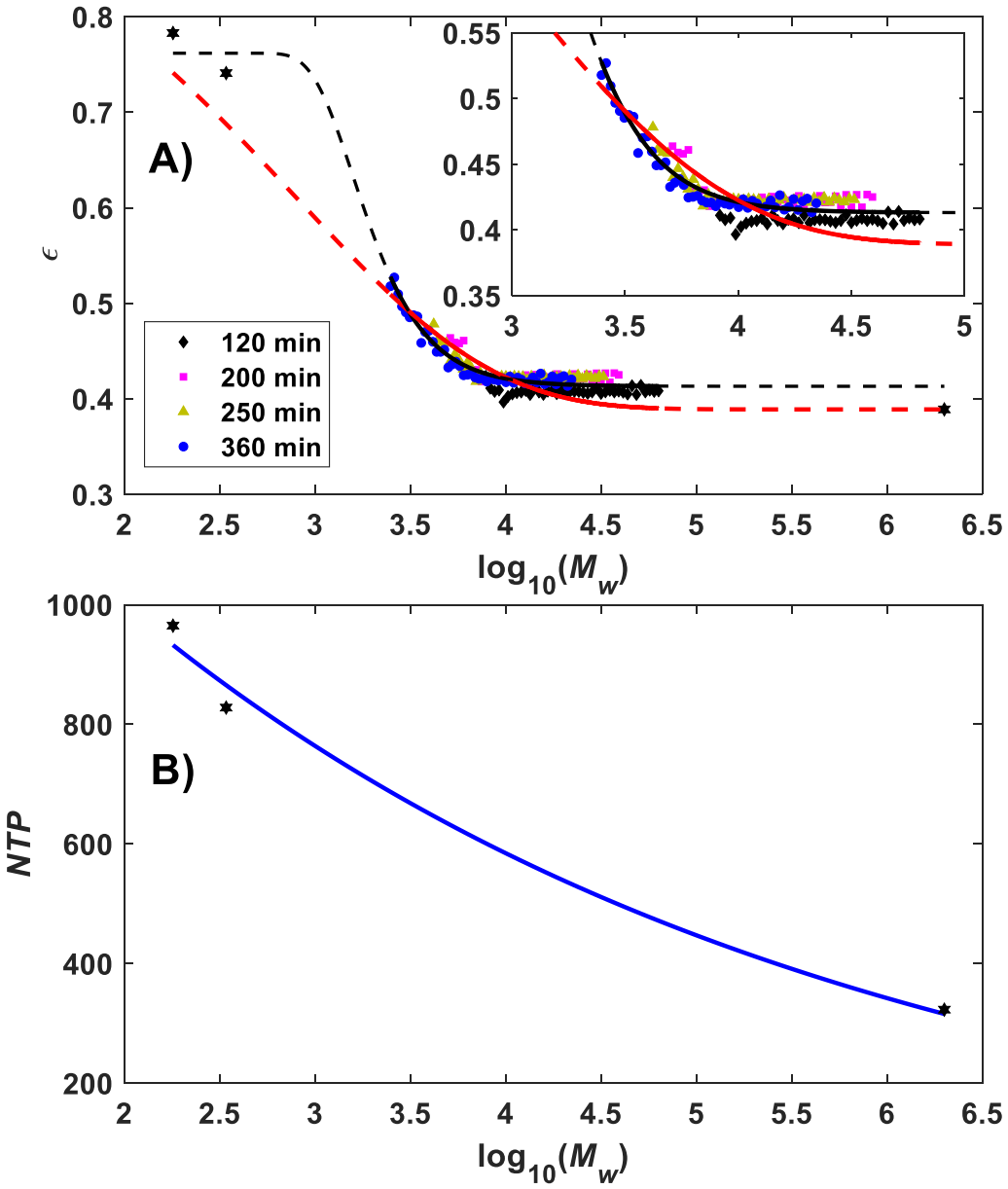


***Figure 2.*** Dependency of the apparent porosity (A) and the column efficiency (B) on the molar mass of *β*–glucan polysaccharides in the preparative SEC column. Hydrolysis times: diamond = 120 min, square = 200 min, triangle = 250 min, circle = 360 min. Data from pure model

substances (glucose, cellobiose, blue dextran) are marked with hexagram. Black and red lines are calculated with Model I and Model II, respectively.

**Table 2.** Parameters of the empirical correlations for apparent porosity and column efficiency.

| **Property** | **Equation** | **Parameters** | | | |
|---|---|---|---|---|---|
| $\overline{\varepsilon}$ **,** Model I | (12) | $a$ | $b$ | $c$ | $d$ |
| | | 0.762 | 0.458 | $3.095\times10^{6}$ | 4.672 |
| $\overline{\varepsilon}$ **,** Model II | (13) | $\gamma$ | $\omega$ | $\lambda$ | |
| | | 4.028 | 0.419 | 1.015 | |
| *NTP* | (14) | $\varphi$ | $\sigma$ | | |
| | | 1705.5 | 0.116 | | |

The *NTP* could be calculated directly from the experimental data for the three model compounds (glucose, cellobiose, and blue dextran) only. The parameters of the *NTP* correlation (Table 2) were estimated by applying the inverse method to the chromatograms measured for the four batches of hydrolysates. As seen in Fig. 2B, the *NTP* correlation is in good agreement with the experimental observations. The experimental and simulated chromatograms of the $\beta$–glucan hydrolysates are displayed in Fig. 3. Overall, the simulation accuracy using the convolution approach is satisfactory, especially considering that there are thousands of individual compounds and simple empirical correlations used for the apparent porosity and the column efficiency.

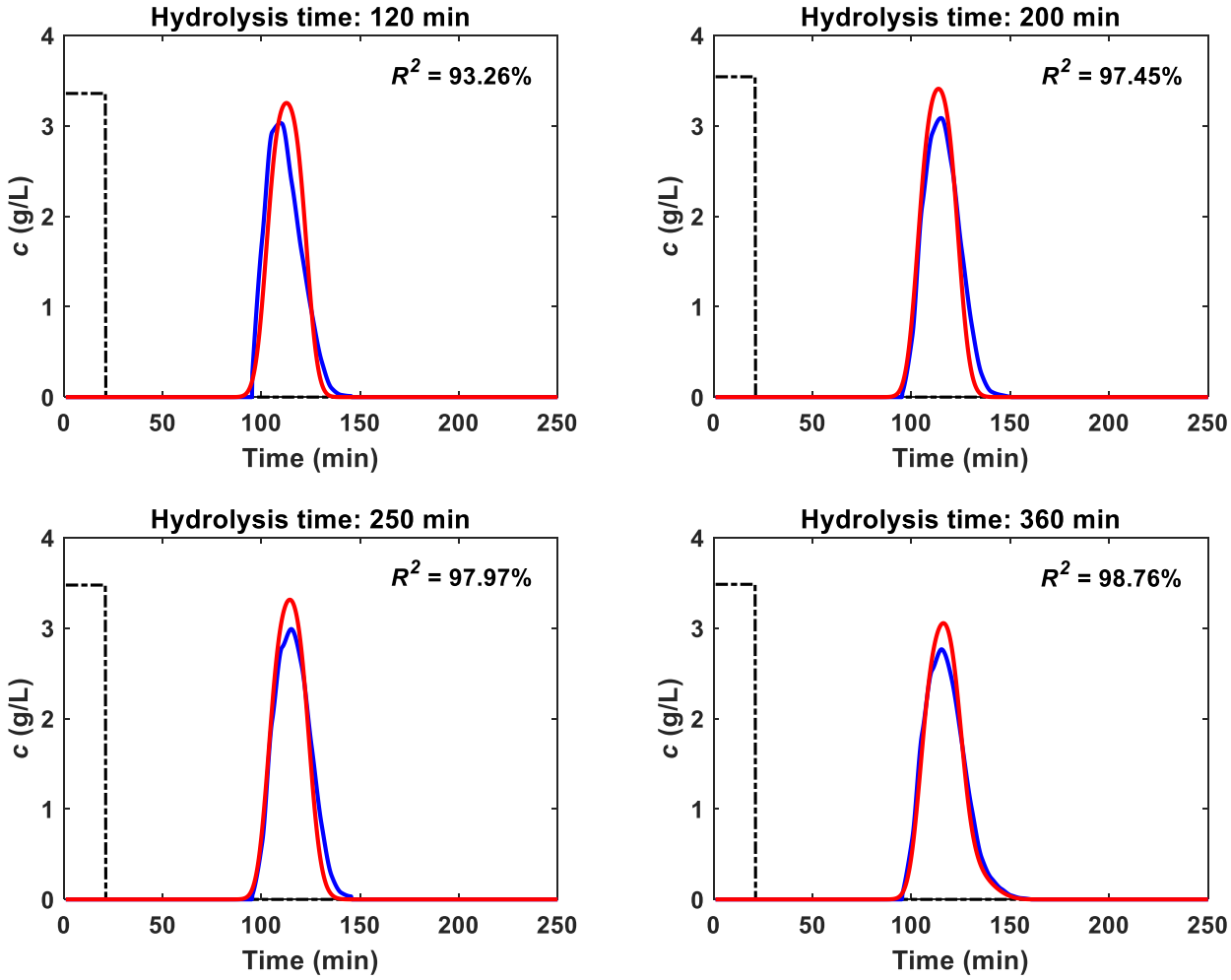


**Figure 3.** Chromatograms of $\beta$–glucan hydrolysates obtained with the preparative SEC column. Dashed-dot line = feed profile, blue solid line = experimental chromatogram, red solid line = simulated chromatogram.

### *4.2. Intermitted recycle-integrated reactor-separator system*

A laboratory scale intermittent reactor-separator with reactor to separator volume ratio $v$ = 0.162 was operated for 7 cycles. The fraction of solution withdrawn on each cycle was $\phi \approx$ 0.25. Due to a limitation of operating pressure in the preparative SEC column, $t_{cycle}$ was chosen as 60 min, which corresponds to $t_{mean}$ = 4 h. Evolution of yield and purity of the target molecules (*DP* = 15–30) in the experiment are shown in Fig. 4. The yield and purity are relatively low,

mainly due to short mean residence time and suboptimal fractionation of the SEC column effluent (see Fig. S1 and Table S2 in Supplementary material). Nevertheless, yield and purity in the intermittent reactor-separator are approximately 2.0 and 2.5 times higher than those obtained experimentally in batch reactor with the same mean residence time ($Y_{BR} = Pu_{BR} \approx 0.04$ after 4 h). The purpose of this experimental run was not to optimize the equipment configuration or the operating parameters but to ensure that the models presented above describe the performance at least qualitatively correctly. The match between the simulation model and the experimental data is good considering that it is a prediction with parameters determined in independent experiments. This gives a good basis for a parametric analysis of the intermittent reactor-separator using numerical simulations.

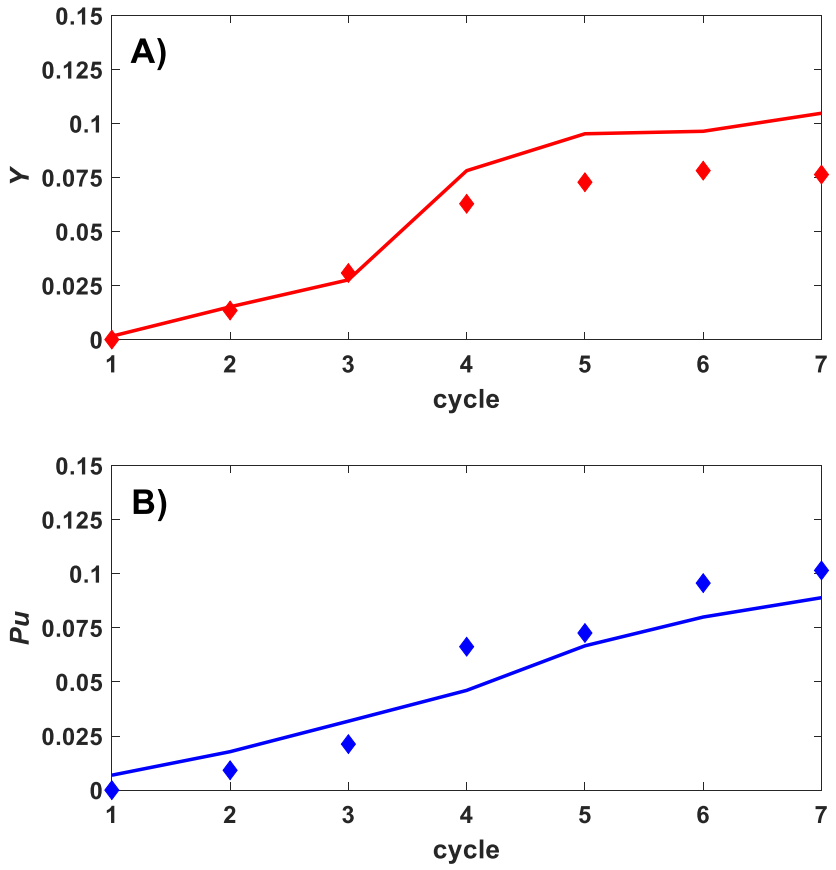

**Figure 4.** Evolution of *Y* (A) and *Pu* (B) of *β*–glucan oligosaccharides with *DP* 15–30 in an intermittent laboratory scale reactor-separator with $\nu$ = 0.162 and $\phi$ = 0.25, $t_{cycle}$ = 60 min. Symbols present experimental data and lines simulated results.

To understand the behavior of the intermittent reactor-separator process in more detail, an extensive simulation study was carried out (no experiment data included). The mean residence time in the reactor ($t_{mean}$), the equipment volume ratio ($\nu$), and the fraction of solution withdrawn per cycle ($\phi$) were varied over a wide range. In each operating point, the cycle time applied was calculated as $t_{cycle} = \phi t_{mean}$. The efficiency of the chromatographic separation column (*NTP*) was assumed independent of the flow rate and column diameter. Flow rate and column diameter were chosen in each operating point such that the separation operation could be completed in exactly one $t_{cycle}$. The concentration of the acid catalyst in the reactor was kept constant.

The effluent from the SEC column was split into four fractions as shown in Fig. 5. The recycle fraction was chosen such that the amount of reactants recycled was maximized. In order to prevent flooding of the reactor, one must set the volume of solution withdrawn from and recycled to the reactor identical. Owing to limited column efficiency, concentration fronts are broader at the outlet than at the inlet. A waste fraction had to be collected and discarded before the recycle fraction to keep the reactor from flooding. The product fraction was collected immediately after the recycle fraction. Its width was chosen such that the recovery yield of the products was maximized. Finally, the impurities were collected in a second waste fraction.

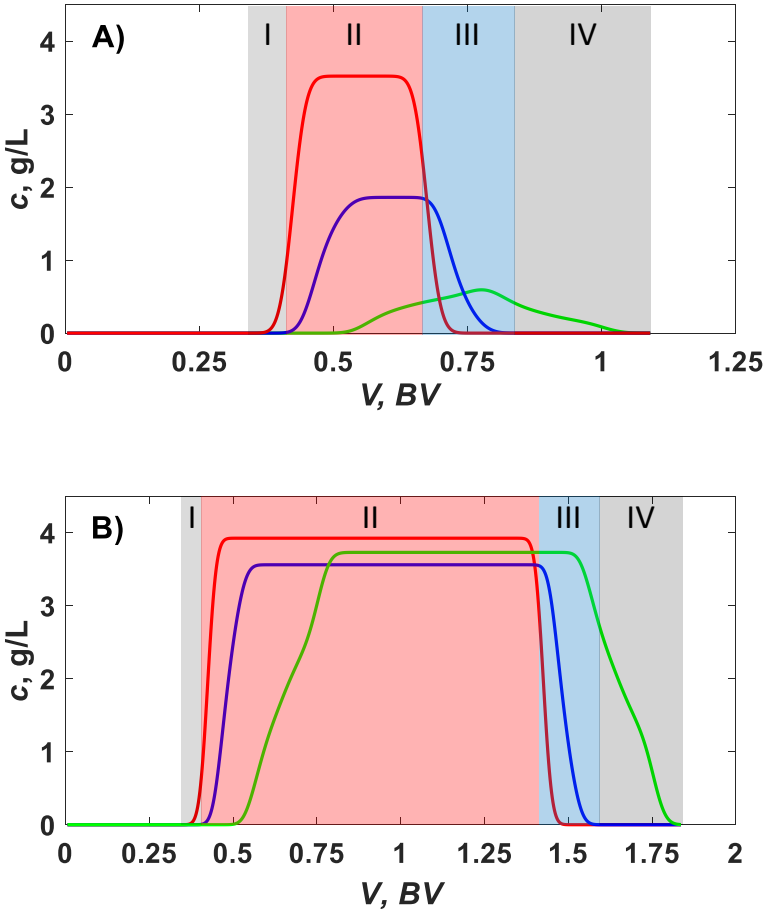


**Figure 5.** Fractionation scheme for the effluent of the SEC column in the intermittent reactor-separator. I and IV are waste fractions, II is the recycle and III is the product fraction. Column loading: (A) $v\phi$ = 0.25, (B) $v\phi$ = 1.0. Reaction conditions: $c_{HCl}$ = 0.05 M, $T$ = 80 °C, $t_{mean}$ = 240 min, $\phi$ = 1. Line colors: red = reactants ($DP$ > 30), blue = target ($DP$ = 15–30), green = impurities ($DP$ < 15).

The productivity of the intermittent reactor-separator, calculated assuming different relative costs of the reactor and separator, is shown in Fig. 6. The curves present the maximum productivity that is achieved for several combinations of $t_{mean}$ and $\phi$ by optimizing $v$. A short

mean residence time is beneficial for productivity simply because the time-average feed rate of $\beta$–glucan increases with decreasing $t_{mean}$.

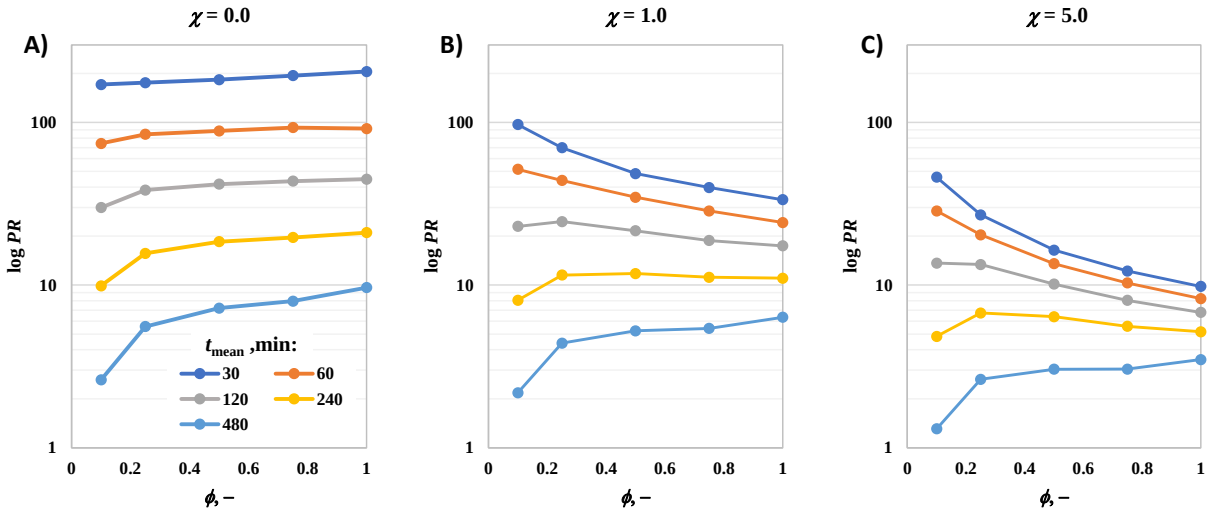


**Figure 6.** Productivity of the intermittent reactor-separator in production of oligosaccharides with *DP* = 15–30 by depolymerization of oat $\beta$–glucan. Reaction conditions: $T$ = 80 °C, $c_{R,HCl}$ = 0.05 mol/L, $c^0_{R,BG}$ = 10 g/L. Separation in a Sephadex G–25 column at $T$ = 60 °C.

If the size of the separator is not considered in calculation of productivity ($\chi$ = 0, Fig. 6A), maximum *PR* is reached at $\phi$ = 1. This is because the intermittent process approaches a serial connection of a batch reactor and SEC separation when the fraction of solution withdrawn on each cycle approaches unity. The polysaccharide hydrolysis reaction is of first order with respect to $\beta$–glucan (at constant acid catalyst concentration), and it is well-known that a batch reactor ($\phi$ = 1) yields a higher conversion than an ideal CSTR ($\phi$ = 0) for reaction systems of this type.

When the reactor and the separator are given equal weight in the productivity function ($\chi$ = 1, Fig. 6B), *PR* behaves differently for high and low values of $t_{mean}$. Batch reactor like operation is preferred at long mean residence times and CSTR like operation is preferred at short mean residence times. This is explained by considering the two functions of the separator, namely recycling unreacted large molecules and recovering the products. If the mean residence time is short, the conversion in the reactor to the target *DP* range is low, and the main task of the separator is to recycle the reactants to increase conversion. As observed by comparing the chromatograms in Fig. 5A and B, the larger the product $V_{col}^{F}/V_{col} = \phi\nu$, the larger fraction of the mass fed to the SEC column is recycled back to the reactor. The separator should not be made infinitely small relative to the reactor (*i.e.*, there is a finite optimum value of $\nu$), however, because a certain degree of separation is needed to recover the product. With a long mean residence time, in contrast, recovering the products becomes an increasingly important function of the separator. The lower the product $\phi\nu$, the better is the separation between molecules of different size, and the higher is the recovery of products.

When operating the separator is made increasingly more costly than operating the reactor by increasing $\chi$ (see Fig. 6C for $\chi$ = 5), the situation remains qualitatively similar to $\chi$ = 1, but the absolute value of productivity of course decreases.

Since the definition of productivity used here includes the equipment volume ratio, *PR* and *Y* may not be optimized at same operating parameter values. Fig. 7A and C display the yield at relatively short (60 min) and long (480 min) mean residence times over a wide range of $\nu$ and $\phi$. (More data is shown in Fig. S2 in Supplementary Document.) In the $t_{mean}$ range studied here, the highest yield of molecules with *DP* = 15–30 is always obtained by operating the reactor as a batch reactor ($\phi$ = 1) and choosing a proper equipment volume ratio. The longer the mean

residence time, the lower equipment volume ratio must be used to maximize yield. To give an example, the highest yield is obtained at $v$ = 0.8 for $t_{mean}$ = 60 min and $v$ = 0.1 for $t_{mean}$ = 480 min. To the left of the optimum $v$, yield becomes low because a large amount of reactants is lost in the first waste fraction. To the right of the optimum, the yield decreases because the recycling rate of product molecules increases, and their probability of being depolymerized into the impurities becomes higher.

Yield and purity of the target molecules are more closely linked than yield and productivity (Fig. 7B and D). It is noteworthy, however, that high purity can be obtained at lower values of $\phi$ than high yield. Inspection of the *Pu* contour lines shows that they often follow closely the $\phi v$ isolines. This is a direct indication of the role of the SEC separation column on product quality. Since $NTP_j$ is taken independent of column aspect ratio and flow rate, separation efficiency depends on the volume of the feed relative to the size of the column only. This ratio is constant along the dashed isolines in Fig. 7B and D, and explains why high purity region extends to lower $\phi$ values.

The majority of literature on reactor-separators focuses on CSTR-based continuous processes [18,20,24]. The results presented above indicate that this may be suboptimal for first-order reactions. When high yield of target products is required, an intermittent operation where a batch reactor is coupled with a separator should be considered. Continuous operation of such system can be achieved with a buffer tank between the reactor and the separator.

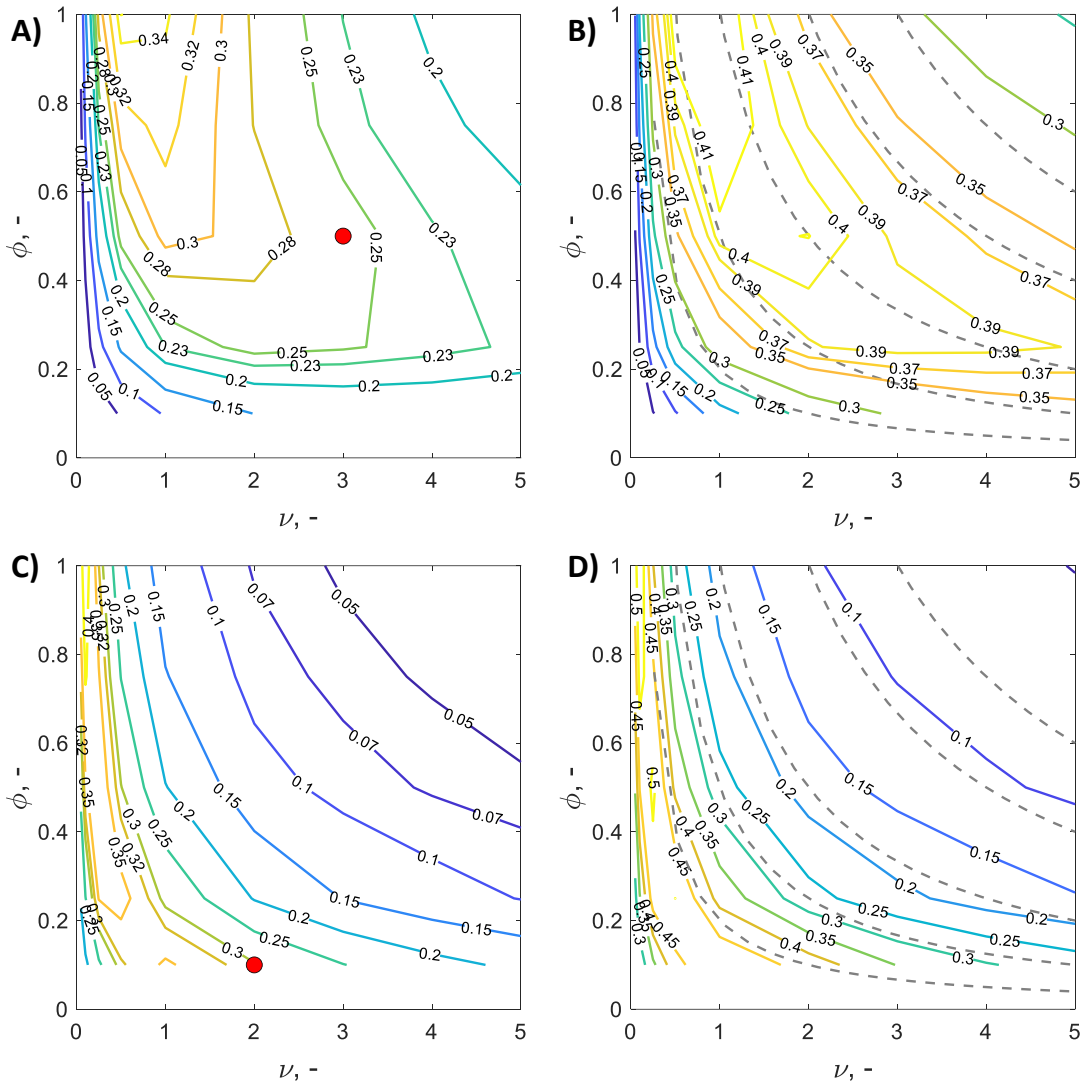


**Figure 7.** Yield (A, C) and purity (B, D) of target molecules (*DP* = 15 – 30) in intermittent reactor-separator. $t_{mean}$ = 60 min in A and B; $t_{mean}$ = 480 min in C and D. Red circles in A and C mark location of maximum productivity with $\chi$ = 1. Dashed lines in B and D indicate constant $\nu\phi$; from top-right to lower-left: $\nu\phi$ = 3.0, 2.0, 1.0, 0.5, 0.2. Reaction conditions as in Fig. 6.

## 5. Conclusion

A new approach to produce non-digestible oligosaccharides with controlled degree of polymerization via acid-catalyzed degradation of oat beta-glucan was studied experimentally and based on numerical simulations. An intermittent recycle-integrated reactor-separator was

used. The experimental results show that with a 4 h mean residence time, the reactor-separator achieved approximately two times higher yield than a stand-alone batch reactor. The purity of target product fraction (*DP* = 15–30) was approximately 2.5 times higher. For future investigations, an automated process appears desirable that enables attaining steady state operation.

The simulations revealed that intermittent operation offers higher yield and product purity than continuous operation (CSTR and chromatographic separation) when mean residence time in the reactor is long. Continuous operation is better when productivity is maximized by using short mean residence time and low yield. Based on the simulations, up to 50% yield and purity of non-digestible oligosaccharides in such narrow target *DP* could be obtained in an intermittent integrated system. Further optimization potential is likely to arise when considering the reaction temperature as an additional variable.

The models used and developed in this work were validated by experimental observations. They could be used to predict the formation and separation of oat beta-glucan polysaccharides and oligosaccharides of any size. The approach based on dimensionless operating and equipment design parameters introduced here could be used for other reactor types as well. For example, a tubular reactor with partial recycling of the outlet could be used to adjust the residence time distribution of molecules before the separator.

**Acknowledgment**

The authors wish to acknowledge CSC – IT Center for Science, Finland, for computational resources. H.N and T.S gratefully acknowledge financial support from the Academy of Finland

(project ID 298229). M.K. was funded by the Deutsche Forschungsgemeinschaft (DFG, German Research Foundation) – Project-ID 416229255 – SFB 1411.

## NOMENCLATURE

### Lattin letters

| | | |
|---|---|---|
| $A$ | cross-sectional area of a chromatographic column, $cm^2$ |
| $a$ | adjustable parameter in Gompertz equation, − |
| $b$ | adjustable parameter in Gompertz equation, − |
| $c$ | concentration, g/L or mol/L |
| $c$ | adjustable parameter in Gompertz equation, − |
| $D_{ax}$ | axial dispersion, $m^2/s$ |
| $\bar{D}$ | apparent dispersion, $m^2/s$ |
| $d$ | adjustable parameter in Gompertz equation, − |
| $DP$ | degree of polymerization, − |
| $H$ | a slope of the linear isotherm |
| $k$ | reaction rate constant, L/mol/s |
| $L$ | height of a chromatographic column, m |
| $M_w$ | molar mass, g/mol |
| $NTP$ | number of theoretical plates, − |
| $PR$ | productivity, kg/L/day |
| $Pu$ | purity, − |
| $Q$ | flow rate, L/s |
| $T$ | temperature, K |
| $t$ | time, min |
| $u$ | linear velocity, m/s |
| $V$ | volume, L |

| | | |
|---|---|---|
| $Y$ | yield, − |

***Superscripts***

| | |
|---|---|
| F | feed into a chromatographic column |
| FF | fresh feed of oat $\beta$–glucan |
| P | product fraction |
| R | recycle fraction |
| W | waste fraction |

***Subscripts***

| | |
|---|---|
| BG | oat $\beta$–glucan |
| col | chromatographic column |
| $j$ | species index |
| R | reactor |
| s | solid phase |
| tot | total |

***Greek letters***

| | |
|---|---|
| $\alpha$ | adjustable parameter in kinetic model, − |
| $\beta$ | adjustable parameter in kinetic model, − |
| $\gamma$ | adjustable parameter in Ogston model, − |
| $\delta$ | distance of a bond from the nearest chain end, − |
| $\overline{\varepsilon}$ | apparent porosity, − |
| $\varepsilon_b$ | bed porosity, − |
| $\lambda$ | adjustable parameter in Ogston model, − |

| | | |
|---|---|---|
| 1 | $v$ | rector to separator volume ratio, − |
| 2 | $\tau$ | space-time in CSTR, dimensionless time in column, – |
| 3 | $\sigma$ | adjustable parameter in NTP correlation, − |
| 4 | $\varphi$ | adjustable parameter in NTP correlation, − |
| 5 | $\phi$ | fraction of solution withdrawn from reactor, − |
| 6 | $\omega$ | adjustable parameter in Ogston model, − |
| 7 | | |
| 8 | | |
| 9 | | |

## References


[1] H.S.H. Nguyen, J. Heinonen, T. Sainio, Acid hydrolysis of glycosidic bonds in oat β-glucan and development of a structured kinetic model, AIChE J. 64 (2018) 2570–2580. https://doi.org/10.1002/aic.16147.

[2] M. Henrion, C. Francey, K.-A. Lê, L. Lamothe, Cereal B-Glucans: The Impact of Processing and How It Affects Physiological Responses, Nutrients. 11 (2019) 1729. https://doi.org/10.3390/nu11081729.

[3] J.M.W. Wong, R. de Souza, C.W.C. Kendall, A. Emam, D.J.A. Jenkins, Colonic health: fermentation and short chain fatty acids., J. Clin. Gastroenterol. 40 (2006) 235–43. http://www.ncbi.nlm.nih.gov/pubmed/16633129.

[4] P.J. Wood, Cereal β-glucans in diet and health, J. Cereal Sci. 46 (2007) 230–238. https://doi.org/10.1016/j.jcs.2007.06.012.

[5] Q. Wang, P.R. Ellis, Oat β-glucan: physico-chemical characteristics in relation to its blood-glucose and cholesterol-lowering properties, Br. J. Nutr. 112 (2014) S4–S13. https://doi.org/10.1017/S0007114514002256.

[6] R.A. Othman, M.H. Moghadasian, P.J. Jones, Cholesterol-lowering effects of oat β-glucan, Nutr. Rev. 69 (2011) 299–309. https://doi.org/10.1111/j.1753-4887.2011.00401.x.

[7] T.M. Wolever, S.M. Tosh, A.L. Gibbs, J. Brand-Miller, A.M. Duncan, V. Hart, B. Lamarche, B.A. Thomson, R. Duss, P.J. Wood, Physicochemical properties of oat β-glucan influence its ability to reduce serum LDL cholesterol in humans: a randomized clinical trial, Am. J. Clin. Nutr. 92 (2010) 723–732. https://doi.org/10.3945/ajcn.2010.29174.

[8] A. Ajithkumar, R. Andersson, P. Åman, Content and Molecular Weight of Extractable β-Glucan in American and Swedish Oat Samples, J. Agric. Food Chem. 53 (2005) 1205–1209. https://doi.org/10.1021/jf040322c.

[9] M. Roberfroid, J. Slavin, Nondigestible Oligosaccharides, Crit. Rev. Food Sci. Nutr. 40 (2000) 461–480. https://doi.org/10.1080/10408690091189239.

[10] P.D. Meyer, Nondigestible Oligosaccharides as Dietary Fiber, J. AOAC Int. 87 (2004) 718–726. https://doi.org/10.1093/jaoac/87.3.718.

[11] S.I. Mussatto, I.M. Mancilha, Non-digestible oligosaccharides: A review, Carbohydr. Polym. 68 (2007) 587–597. https://doi.org/10.1016/j.carbpol.2006.12.011.

[12] R.D. Singh, J. Banerjee, A. Arora, Prebiotic potential of oligosaccharides: A focus on xylan derived oligosaccharides, Bioact. Carbohydrates Diet. Fibre. 5 (2015) 19–30. https://doi.org/10.1016/j.bcdf.2014.11.003.

[13] O. Kodo, Functional Oligosaccharide and Its New Aspect as Immune Modulation, J. Biol. Macromol. 6 (2006) 3–9.

[14] H.S.H. Nguyen, J. Heinonen, M. Laatikainen, T. Sainio, Evolution of the molar mass distribution of oat β-glucan during acid catalyzed hydrolysis in aqueous solution, Chem. Eng. J. 382 (2020) 122863. https://doi.org/10.1016/j.cej.2019.122863.

[15] Y. Qin, J. Xie, B. Xue, X. Li, J. Gan, T. Zhu, T. Sun, Effect of acid and oxidative degradation on the structural, rheological, and physiological properties of oat β-glucan, Food Hydrocoll. (2020) 106284. https://doi.org/10.1016/j.foodhyd.2020.106284.

[16] J.C. Cabrera, P. Van Cutsem, Preparation of chitooligosaccharides with degree of polymerization higher than 6 by acid or enzymatic degradation of chitosan, Biochem. Eng. J. 25 (2005) 165–172. https://doi.org/10.1016/j.bej.2005.04.025.

[17] M. Chemin, A.-L. Wirotius, F. Ham-Pichavant, G. Chollet, D. Da Silva Perez, M. Petit-Conil, H. Cramail, S. Grelier, Well-defined oligosaccharides by mild acidic hydrolysis of hemicelluloses, Eur. Polym. J. 66 (2015) 190–197. https://doi.org/10.1016/j.eurpolymj.2015.02.008.

[18] T. Sainio, M. Kaspereit, Analysis of reactor–separator processes for polymeric and oligomeric degradation products with controlled molar mass distributions, Chem. Eng. Sci. 229 (2021) 116154. https://doi.org/10.1016/j.ces.2020.116154.

[19] A. Nath, C. Bhattacharjee, R. Chowdhury, Synthesis and separation of galacto-oligosaccharides using membrane bioreactor, Desalination. 316 (2013) 31–41. https://doi.org/10.1016/j.desal.2013.01.024.

[20] Q. Gan, S.. Allen, G. Taylor, Design and operation of an integrated membrane reactor for enzymatic cellulose hydrolysis, Biochem. Eng. J. 12 (2002) 223–229. https://doi.org/10.1016/S1369-703X(02)00072-4.

[21] S. Al-Zuhair, M. Al-Hosany, Y. Zooba, A. Al-Hammadi, S. Al-Kaabi, Development of a membrane bioreactor for enzymatic hydrolysis of cellulose, Renew. Energy. 56 (2013) 85–89. https://doi.org/10.1016/j.renene.2012.09.044.

[22] A.K. Goulas, J.M. Cooper, A.S. Grandison, R.A. Rastall, Synthesis of isomaltooligosaccharides and oligodextrans in a recycle membrane bioreactor by the combined use of dextransucrase and dextranase, Biotechnol. Bioeng. 88 (2004) 778–787. https://doi.org/10.1002/bit.20257.

[23] K. Pocedičová, L. Čurda, D. Mišún, A. Dryáková, L. Diblíková, Preparation of galacto-oligosaccharides using membrane reactor, J. Food Eng. 99 (2010) 479–484. https://doi.org/10.1016/j.jfoodeng.2010.02.001.

[24] O. Filo, S. Guzy, S. Sivan, S. Sideman, N. Lotan, Process analysis of a reactor-separator system: Enzymic degradation of polymeric substrates, Isr. J. Chem. 45 (2005) 495–505. https://doi.org/10.1560/4R47-L33A-43GU-AAVC.

[25] A. Andersson, T. Persson, G. Zacchi, H. Stålbrand, A.-S. Jönsson, Comparison of diafiltration and size-exclusion chromatography to recover hemicelluloses from process water from thermomechanical pulping of spruce, Appl. Biochem. Biotechnol. 137–140 (2007) 971–983. https://doi.org/10.1007/s12010-007-9112-9.

[26] S.M. Tosh, P.J. Wood, Q. Wang, J. Weisz, Structural characteristics and rheological properties of partially hydrolyzed oat β-glucan: the effects of molecular weight and hydrolysis method, Carbohydr. Polym. 55 (2004) 425–436. https://doi.org/10.1016/j.carbpol.2003.11.004.

[27] W. Li, S.W. Cui, Q. Wang, R.Y. Yada, Studies of aggregation behaviours of cereal β-glucans in dilute aqueous solutions by light scattering: Part I. Structure effects, Food Hydrocoll. 25 (2011) 189–195. https://doi.org/10.1016/j.foodhyd.2010.02.005.

[28] Y. Brummer, C. Defelice, Y. Wu, M. Kwong, P.J. Wood, S.M. Tosh, Textural and Rheological Properties of Oat Beta-Glucan Gels with Varying Molecular Weight Composition, J. Agric. Food Chem. 62 (2014) 3160–3167. https://doi.org/10.1021/jf405131d.

[29] O. Levenspiel, The dispersion model, in: Chem. React. Eng., 3rd ed., John Wiley & Sons, Ltd, 1999: pp. 293–320.

[30] A. Seidel-Morgenstern, H. Schmidt-Traub, M. Michel, A. Epping, A. Jupke, Modeling and Model Parameters, in: Prep. Chromatogr., John Wiley & Sons, Ltd, 2013: pp. 321–424. https://doi.org/10.1002/9783527649280.ch6.

[31] B. Kalbfuss, D. Flockerzi, A. Seidel-Morgenstern, U. Reichl, Size-exclusion chromatography as a linear transfer system: Purification of human influenza virus as an example, J. Chromatogr. B. 873 (2008) 102–112. https://doi.org/10.1016/j.jchromb.2008.08.002.

[32] R.-M. Nicoud, Fluid–solid phase equilibria, in: Chromatogr. Process., Cambridge University Press, Cambridge, 2015: pp. 139–215. https://doi.org/10.1017/CBO9781139998284.005.

[33] J.C. Bosma, J.A. Wesselingh, Partitioning and diffusion of large molecules in fibrous structures, J. Chromatogr. B Biomed. Sci. Appl. 743 (2000) 169–180. https://doi.org/10.1016/S0378-4347(00)00134-1.